

Combined *in situ* conductivity and Raman studies of rubidium doping of single-wall carbon nanotubes

N. Bendiab,¹ L. Spina,¹ A. Zahab,¹ P. Poncharal,¹ C. Marlière,² J. L. Bantignies,¹ E. Anglaret,¹ and J. L. Sauvajol¹

¹Groupe de Dynamique des Phases Condensées, UMR CNRS 5581, Université Montpellier II, 34095 Montpellier Cedex 5, France

²Laboratoire des Verres, UMR CNRS 5587, Université Montpellier II, 34095 Montpellier Cedex 5, France

(Received 21 September 2000; revised manuscript received 11 December 2000; published 28 March 2001)

Phase transitions and staging in doped single-wall carbon nanotubes (SWNT's) are controversial issues. Here, we report on combined *in situ* conductivity and Raman measurements of Rb-doped SWNT's. Striking correlations between resistance, changes of resistance under laser irradiation, and frequency of the main Raman peak are observed. In the last steps of doping, two different Raman signatures, with peaks at 1596 and 1555 cm^{-1} , respectively, are observed and assigned to two different stable doped phases. The two phases coexist in a specific range of doping with the latter growing progressively at the expense of the former.

DOI: 10.1103/PhysRevB.63.153407

PACS number(s): 78.30.Na, 61.48.+c

All-carbon lattices can form intercalated synthetic metals by chemical doping. This has been extensively investigated for graphite (GIC's) and fullerene intercalated compounds (FIC's) (Refs. 1 and 2), and was also demonstrated recently for single-wall carbon nanotubes (SWNT's).^{3–15} The transport properties of bundles of SWNT's were shown to be drastically changed by alkali-metal doping.^{3–7} However, no evidence for the existence of different stable phases was reported in doped SWNT's,^{12,15} in contrast with GIC's where several "stages" have been observed,¹ or FIC's where different well-defined stoichiometries and structures have been elucidated (A_xC_{60} with $A = K, Rb, Cs$ and $x = 1–6$).² Electron transfer and the metallic character of doped SWNT's have also been probed by Raman scattering.^{8,9} Saturation-doped compounds feature a main, broad, and asymmetric peak in the range 1540–1565 cm^{-1} assigned to tangential modes (TM's) of the doped carbon atoms, a set of symmetric peaks in the range 900–1500 cm^{-1} , and two weak features in the low-frequency range around 50 and 180 cm^{-1} , assigned to modes involving both radial motions of the carbons and vibrations of the alkali-metal atoms.⁹ Since Raman spectroscopy is sensitive to both structural changes and electron transfer processes, this technique might provide valuable information on the mechanisms and kinetics of doping. Here, we report on coupled *in situ* conductivity and Raman investigations of a rubidium-doped SWNT mat. The global semi-conducting or metallic character of the mat is probed by the conductivity measurements. Striking correlations are evidenced between the time dependence of resistance and the Raman profile. These experiments allow us to describe the different steps of doping and to identify two stable phases for Rb-doped SWNT's.

SWNT collarets are prepared by the electric-arc technique as detailed in Ref. 16. The samples are purified in a four-step method, namely, reflux in nitric acid, dispersion in a surfactant solution, filtration and annealing in vacuum at 1200 °C for 24 h. The final product is a compact "mat," with most of the tubes assembled into crystalline bundles, as shown by electron microscopy¹⁶ and diffraction experiments.^{16,17} The distribution of tube diameters can be estimated to be about 1.4 ± 0.2 nm. After outgassing and annealing of the sample

at 200 °C for 24 h, doping in the vapor phase is achieved in a Pyrex chamber under dynamical vacuum by heating a piece of rubidium at 150 °C in a first step and at 200 °C in a second step. A gradient of temperature of about 20 °C is imposed between the alkali-metal reservoir and the sample in order to prevent alkali-metal condensation on the sample. The mat resistance is measured with a four-probe setup. Raman spectra are excited with the green line (2.41 eV) of an Ar laser and recorded using a triple monochromator Jobin-Yvon T64000 spectrometer in a backscattering configuration every 4 min during the whole experiment (the acquisition time is 2 min for each spectrum).

Figure 1 (solid line) displays the time dependence of the resistance of the SWNT mat, with $t=0$ corresponding to the

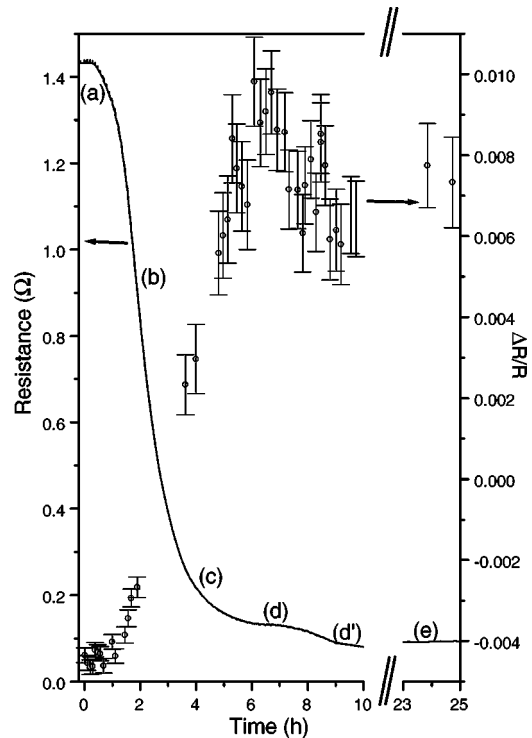


FIG. 1. Evolution of the mat resistance R and $\Delta R/R$ during the doping experiment (solid line and symbols, respectively).

time when the rubidium container is broken and the temperature kept at 150 °C. After 6 h, the resistance has fallen by approximately a factor of 10 and the first plateau is observed. At $t=8$ h, the temperature increase from 150 to 200 °C in order to accelerate the reaction. This leads to another decrease of the resistance down to a minimum reached at about $t=12$ h (not shown). Then, the resistance increases slightly again up to a second plateau to reach a value about 15 times smaller than that of the pristine mat. Note that the two plateaus were also observed in other sets of measurements where the temperature was kept constant throughout the experiment. The change of resistance of the sample when exposed to the laser beam is a striking feature. Assuming it is a pure thermal effect,¹⁰ $\Delta R = R_{laser} - R_{darkness}$ is directly related to dR/dT . Consequently, ΔR is expected to be negative (positive) for semiconducting (metallic) samples. For a mat, R and ΔR reflect at a macroscopic scale the contributions of both semiconducting and metallic domains, intrinsic (semiconducting and metallic bundles and SWNT's) and extrinsic (traces of impurities, contacts). Assuming that only intrinsic contributions are modified by doping, the time dependence of R and ΔR is a good probe of the growth (loss) of metallic (semiconducting) SWNT domains in the samples (Fig. 1). In the pristine mat (at $t=0$) ΔR is negative, indicating a global semiconducting character. During the first 6 h of doping, $\Delta R/R$ increases almost linearly and becomes positive after about 3 h. A maximum is reached at about 6.5 h, which corresponds to the first plateau of conductivity. Finally, $\Delta R/R$ decreases slightly to reach a second plateau at a positive value at the end of the experiment, indicating a global metallic character of the doped samples. This metallic character was confirmed *a posteriori* by measurement of the temperature dependence of the resistance of the doped mat. The results will be presented in detail elsewhere.¹⁰

Figure 2 shows the Raman spectra of the SWNT mat at several doping steps. The laser energy used in the Raman experiments, 2.41 eV, is close to the third allowed optical transition between Van Hove singularities in the electronic density of states of pristine semiconducting nanotubes of diameter 1.4 ± 0.2 nm.^{18–20} The corresponding Raman spectra in the range of the tangential modes displays a symmetric profile with a dominant peak around 1592 cm^{-1} and another structure around 1563 cm^{-1} [Fig. 2, spectrum (a)]. In the low-frequency range, the radial breathing modes (RBM's) are located around 180 cm^{-1} (not shown). The intensity of the RBM's rapidly decreases during doping⁹ and becomes unresolved (within the experimental conditions) after about 2 h. No significant shift of the RBM's was observed. A detailed investigation of the low-frequency range of the Raman spectra of saturation-doped SWNT's is presented elsewhere.⁹ Here, we will focus only on the changes occurring in the TM range during doping. Typical spectra corresponding to points (a) to (e) in Fig. 1 are displayed in Fig. 2. As soon as doping begins, a continuous loss of intensity of the TM's is observed, as well as a broadening of the two main peaks [spectra (a) to (c)]. No significant shift of the main peak is observed between (a) and (c). This first step in the doping reaction corresponds to a continuous decrease of the resistance and a concomitant continuous increase of $\Delta R/R$. From

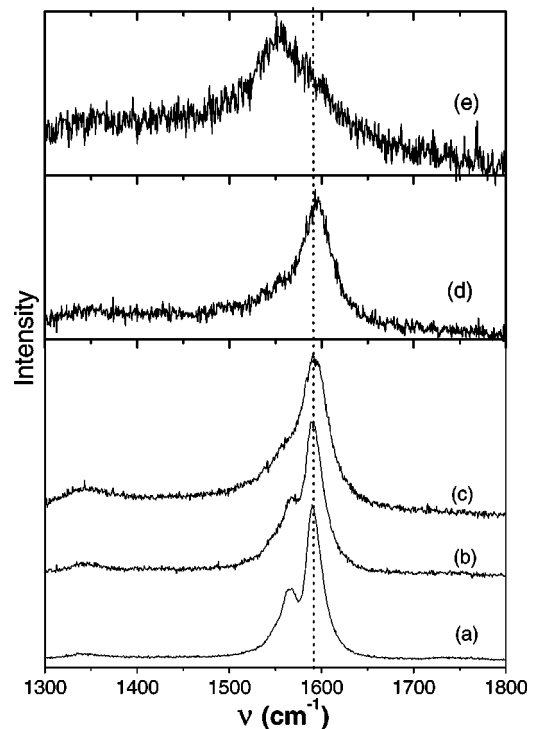


FIG. 2. Evolution of the Raman spectra of the TM during doping. Labels (a) to (e) correspond to different times, as indicated on Fig. 1. The intensities were normalized in order to optimize the comparison of the spectral profiles.

(c) to (d), a progressive (and weak) upshift of the main peak is observed (from 1592 to 1596 cm^{-1}). The TM profile of spectrum (d) features a single and symmetric line and is significantly different from the spectra of both pristine and saturation-doped samples. Spectrum (d) corresponds to the first plateau of conductivity and to the maximum of $\Delta R/R$. The same profile is measured all along the plateau. A comparable upshift was also observed on lithium-doped SWNT's,⁹ prepared electrochemically¹² and by redox reactions.¹⁵ Finally, spectrum (e) is measured at the end of the experiment, when the sample is completely doped. The maximum of the main peak is found to be downshifted to around 1555 cm^{-1} and its profile is very asymmetric. The asymmetry is assigned to Breit-Wigner-Fano interferences between phonons and an electronic continuum, as suggested elsewhere.^{8,9} It is worth studying in detail the evolution of the spectrum between (d) and (e). It is clear from Fig. 3 that the two peaks at about 1555 and 1596 cm^{-1} coexist in several spectra between (d) and (d') with the intensity of the former increasing progressively to the detriment of that of the latter. Spectrum (d') is very close to spectrum (e).

This indicates that the two phases coexist in a specific range of doping and that the saturation-doped phase grows at the expense of phase 1. The range of coexistence corresponds to a slight decrease of $\Delta R/R$, indicating a change in the transport properties of the doped SWNT's between (d) and (e). It is tempting to assign this striking evolution of the Raman profile over a very short decrease of resistance to a first-order structural phase transition between the two stable phases. It is well established that each intrinsic alkali-metal-

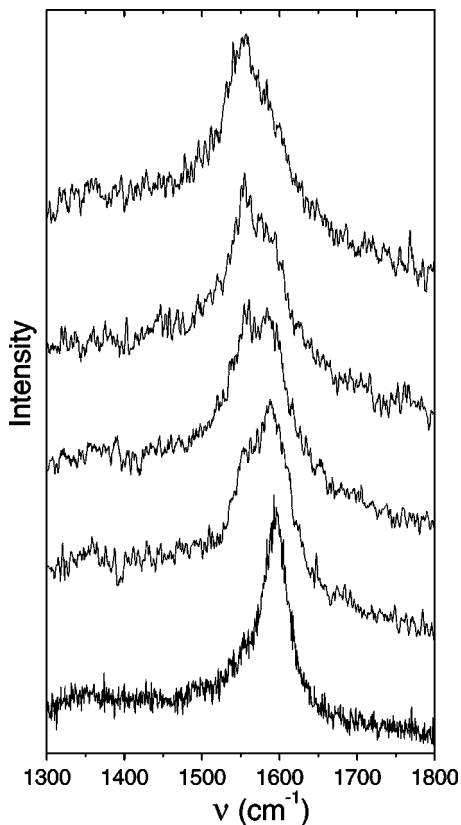


FIG. 3. From bottom to top, evolution of the Raman spectra between (d) and (d'). The intensities were normalized in order to optimize the comparison of the spectral profiles.

doped phase (different stages in GIC's and different stoichiometries in A_xC_{60} compounds) features a specific Raman spectrum. By analogy, we assign spectrum (d) to an intrinsic stable phase of the alkali-metal-doped SWNT. The upshift of the TM's is surprising and needs to be carefully addressed. Indeed, a downshift was systematically observed for saturation alkali-metal-doped samples.^{8,9} In intercalated SWNT doped compounds, two processes might be responsible for the Raman shifts. The first involves changes in the intra- and intertube force constants induced by structural reorganizations of the SWNT-alkali-metal system (expansion or deformation of the hexagonal lattice, hardening of the lattice via tube-alkali-metal interactions, structural disorder, etc). The second process relates to charge transfer, which directly modifies the intratube force constants and leads systematically in all-carbon alkali-metal-doped systems to a softening of the modes involving C-C stretching (E_{2g} graphite mode in GIC's, A_{1g} pentagonal pinch mode in A_xC_{60} compounds, TM in doped SWNT's). Therefore, we assign the upshift observed for this spectrum to a dominant contribution of struc-

tural effects. *In situ* diffraction studies will be necessary to detail the structure of this phase. The spectrum of the second stable alkali-metal-doped phase appears to be that of the saturation-doped SWNT.^{8,9} Here, by contrast with the first phase, the changes in the Raman profile are dominated by the charge transfer effect. The diffraction patterns of saturation-doped samples were reported by Duclaux *et al.*¹⁴ Their data suggest that a large number of rubidium atoms fill the hollow channels of the bundles.

The continuous decrease of Raman intensity during the doping experiment is assigned to a loss of resonance, i.e., to a continuous filling of the electronic states of the semiconducting tubes, in agreement with the *in situ* optical absorption measurements of Ref. 7. However, we emphasize that resonance in semiconducting tubes is expected to be effective until the third singularity of the density of states is completely filled within the frame work of the rigid band model. The broadening of the Raman peaks is likely related to disorder and inhomogeneities induced by the intercalation of alkali-metal atoms.

The Raman changes are associated with three features of the mat conductivity: (i) a continuous decrease of the resistance, (ii) a first plateau of resistance associated with a maximum of $\Delta R/R$ corresponding to phase I, and (iii) a decrease of both the resistance and $\Delta R/R$ down to a second plateau corresponding to phase II. These correlations support our hypothesis that the time dependence of R and ΔR reflects mainly intrinsic SWNT contributions.

A two-phase model was recently proposed by Claye *et al.* for alkali-metal-doped SWNT's using electrochemistry, where doped noncrystalline regions grow at the expense of undoped crystalline regions.¹² This model implies the coexistence of two spectra in Raman experiments, but such a coexistence was not observed in this previous study.¹² In the present experiment, we do observe the coexistence of two phases but our interpretation is different from that of Ref. 12. In the first steps of doping, the nondoped crystalline phase featuring two main Raman peaks around 1563 and 1592 cm^{-1} progressively vanishes while the first doped phase (phase I) grows, showing a single Raman peak around 1596 cm^{-1} . In the last step of doping, the saturation-doped phase (phase II) grows at the expense of phase I and the two phases coexist over a specific range of doping. We assign spectra (d) and (e) to the intrinsic Raman responses of phases I and II, respectively. Structural investigations will be necessary to achieve a complete interpretation of the Raman/conductivity data.

We thank S. Tahir and P. Bernier for providing us with the SWNT samples.

¹M.S. Dresselhaus and G. Dresselhaus, *Adv. Phys.* **30**, 139 (1981), and references therein.

²*Science of Fullerenes and Carbon Nanotubes*, edited by M.S. Dresselhaus, G. Dresselhaus, and P.C. Eklund (Academic Press,

San Diego, 1995), and references therein.

³R.S. Lee, H.J. Kim, J.E. Fischer, A. Thess, and R.E. Smalley, *Nature (London)* **388**, 255 (1997).

⁴L. Grigorian, G.U. Sumanasekera, A.L. Loper, S. Fang, J.L.

- Allen, and P.C. Eklund, Phys. Rev. B **58**, R4195 (1998).
- ⁵R.S. Lee, H.J. Kim, J.E. Fischer, J. Lefebvre, M. Radosavljevic, J. Hone, and A.T. Johnson, Phys. Rev. B **61**, 4526 (2000).
- ⁶M. Bockrath, J. Hone, A. Zettl, P.L. Mac Euen, A.G. Rinzler, and R.E. Smalley, Phys. Rev. B **61**, R10 606 (2000).
- ⁷S. Kazaoui, N. Minami, R. Jacquemin, H. Kataura, and Y. Achiba, Phys. Rev. B **60**, 13 339 (1999).
- ⁸A.M. Rao, P.C. Eklund, S. Bandow, A. Thess, and R.E. Smalley, Nature (London) **388**, 257 (1997).
- ⁹N. Bendiab, A. Righi, E. Anglaret, J.L. Sauvajol, L. Duclanx, and F. Béguin, Chem. Phys. Lett. (to be published).
- ¹⁰A. Zahab *et al.* (unpublished).
- ¹¹A. Claye and J.E. Fischer, Electrochim. Acta **45**, 107 (1999).
- ¹²A.S. Claye, N.M. Nemes, A. Jánossy, and J.E. Fischer, Phys. Rev. B **62**, 4845 (2000).
- ¹³C. Bower, S. Suzuki, K. Tanigaki, and O. Zhou, Appl. Phys. A: Mater. Sci. Process. **67**, 47 (1998).
- ¹⁴L. Duclaux, K. Metenier, J.P. Salvétat, P. Lauginie, S. Bonnamy, and F. Béguin, Mol. Cryst. Liq. Cryst. Sci. Technol., Sect. B **34**, 769 (2000).
- ¹⁵E. Jouguelet, C. Mathis, and P. Petit, Chem. Phys. Lett. **318**, 561 (2000).
- ¹⁶C. Journet, W.K. Maser, P. Bernier, A. Loiseau, M. Lamy de la Chapelle, S. Lefrant, P. Deniard, R. Lee, and J.E. Fischer, Nature (London) **388**, 756 (1997).
- ¹⁷S. Rols, R. Almairac, L. Henrard, E. Anglaret, and J.L. Sauvajol, Eur. Phys. J. B **10**, 263 (1999).
- ¹⁸H. Kataura, Y. Kumazawa, Y. Maniwa, I. Umezu, S. Suzuki, Y. Ohtsuka, and Y. Achiba, Synth. Met. **103**, 2555 (1999).
- ¹⁹M.A. Pimenta, A. Marucci, S.A. Empedocles, M.G. Bawendi, E.B. Hanlon, A.M. Rao, P.C. Eklund, R.E. Smalley, G. Dresselhaus, and M.S. Dresselhaus, Phys. Rev. B **58**, R16 016 (1998).
- ²⁰L. Alvarez, A. Righi, T. Guillard, S. Rols, E. Anglaret, D. Laplaze, and J.-L. Sauvajol, Chem. Phys. Lett. **316**, 186 (2000).